environmental microbiology

Environmental Microbiology (2010) **12**(6), 1734–1747 doi:10.1111/j.1462-2920.2010.02253.x

How *Pseudomonas aeruginosa* adapts to various environments: a metabolomic approach

Eliane Frimmersdorf,[1†] Sonja Horatzek,[2†] Anya Pelnikevich,[2] Lutz Wiehlmann[2‡] and Dietmar Schomburg[1*‡]

[1]*Department of Biochemistry and Bioinformatics, Institute for Biochemistry & Biotechnology, Technische Universitaet Braunschweig, 38106 Braunschweig, Germany.*

[2]*Klinische Forschergruppe, OE 6710, Medizinische Hochschule Hannover, Carl-Neuberg-Str. 1, 30625 Hannover, Germany.*

Summary

In addition to transcriptome and proteome studies, metabolome analysis represents a third complementary approach to identify metabolic pathways and adaptation processes. In order to elucidate basic principles of metabolic versatility of *Pseudomonas aeruginosa*, we investigated the metabolome profiles of two genetically and morphologically divergent strains, the reference strain PAO1 and the mucoid clinical isolate TBCF10839 in exponential growth and stationary phase in six different carbon sources (cadaverine, casamino acids, citrate, glucose, succinate and tryptone). Both strains exhibited strong similarities in mode of growth; the metabolite patterns were mainly defined by the growth condition. Besides this adaptive response, a basic core metabolism shapes the *P. aeruginosa* metabolome, independent of growth phase, carbon source and genetic background. This core metabolism includes pathways related to the central energy and amino acid metabolism. These consistently utilized metabolic pathways are closely related to glutamate which represents a dominant metabolite in all conditions analysed. In nutrient-depleted media of stationary phase cultures, *P. aeruginosa* maintains a specific repertoire of metabolic pathways that are related to the carbon source formerly available. This specified adaptation strategy combined with the invariant basic core metabolism may represent a fundamental requirement for the metabolic versatility of this organism.

Received 28 October, 2009; accepted 15 April, 2010. *For correspondence. E-mail d.schomburg@tu-bs.de; Tel. (+49) 531 391 8301; Fax (+49) 531 391 8302. †E.F. and S.H. contributed equally to this work and should be considered as joint first authors. ‡D.S. and L.W. contributed equally to this work and should be considered as joint last authors.

Introduction

The Gram-negative ubiquitous microorganism *Pseudomonas aeruginosa* exhibits extreme metabolic versatility (Ramos, 2004). *Pseudomonas aeruginosa* colonizes diverse environmental habitats and is able to persist and grow even under nutrient-poor and hostile conditions (Schmidt *et al.*, 1996; OECD, 1997). In addition to environmental habitats, *P. aeruginosa* strains are frequently isolated from clinical sources. As one of the most relevant causative agents of nosocomial infections (Campa *et al.*, 1993) this opportunistic human pathogen establishes acute or chronic infections in hospitalized and immunodeficient patients (Quinn, 2003; Trautmann *et al.*, 2005). Lifestyles of this organism comprise both planktonic growth and alginate-associated biofilm formation (Davies *et al.*, 1993). Successful adaptation to multiple niches requires extraordinary physiological capabilities and reflects the broad metabolic capacity of this organism, which, particularly in low-nutrient conditions, provides distinct advantages for outgrowing competitors (Kiewitz and Tümmler, 2000).

Based on the *P. aeruginosa* PAO1 genome sequence, 8% of the 6.3 Mbp genome is predicted to encode transcriptional regulators and two-component regulatory systems (Anba *et al.*, 1990; Stover *et al.*, 2000; Nishijyo *et al.*, 2001; Krieger *et al.*, 2002). Along with a large number of genes for substrate uptake and catalysis, which enable the bacterium to metabolize various compounds as nutrients, high environmental adaptability is granted (Stanier *et al.*, 1966).

Energy generation is mainly based on oxidative substrate catabolism; however, the bacterium is also able to flourish in a facultative anaerobic environment with alternative external electron acceptors or to survive by fermentation of arginine or pyruvate (Wauven *et al.*, 1984; Davies *et al.*, 1989; Eschbach *et al.*, 2004; Filiatrault *et al.*, 2006; Williams *et al.*, 2007). If a preferred nutrient is offered in a mixture along with unfavoured carbon sources, the carbon metabolism of *P. aeruginosa* is regulated by catabolite repression control, which facilitates catabolism of substrates in an ordered fashion (Suh *et al.*, 2002). Preferentially chosen sources of carbon or nitrogen

include short-chain fatty acids, amino acids and polyamines (Stanier *et al*., 1966; Lessie and Neidhardt, 1967; Meile *et al*., 1982; Tricot *et al*., 1994). Although efficiently metabolized, sugars represent less preferred substrates for *P. aeruginosa*, which are degraded via the Entner-Doudoroff pathway (Entner and Doudoroff, 1952; Goldbourt *et al*., 2007). Growth on *n*-alkanes and (halogenated) aromatic compounds reflects the metabolic potential of *P. aeruginosa* to degrade complex xenobiotics (Palleroni, 1986; Hickey and Focht, 1990; Marín *et al*., 2003). In addition to its remarkable capacity of substrate utilization, *P. aeruginosa* is proficient in extensive secondary metabolite production (Leisinger and Margraff, 1979; Gallagher and Manoil, 2001).

Metabolic competence of *P. aeruginosa* has been previously intensively investigated in many transcriptome studies (Palma *et al*., 2003; Salunkhe *et al*., 2005; Weir *et al*., 2008). Furthermore, using nuclear magnetic resonance technology, a metabolomics approach was employed to study the overall metabolic profiles of *P. aeruginosa* biofilm and planktonic cells (Gjersing *et al*., 2007).

Our study aims to investigate the global regulatory network of the *P. aeruginosa* metabolism with respect to the metabolic proficiency of this organism to cope with diverse habitats. We used a gas chromatography-mass spectrometry (GC-MS)-based approach to assess both intra- and extracellular metabolite spectra (Strelkov *et al*., 2004). Metabolome data were further statistically analysed with pattern recognition tools for the evaluation of metabolic pathway utilization. The resulting global view on the metabolome uncovers new aspects of adaptation processes to environmental conditions and reveals the nature of metabolic versatility in *P. aeruginosa*.

Results and discussion

Selection of growth conditions

We included two genetically and morphologically divergent strains of *P. aeruginosa*, the reference strain PAO1 and the mucoid clinical isolate TBCF10839, in our analyses to investigate strain-specific metabolic features, as well as general aspects of *P. aeruginosa* metabolism. In order to obtain extensive information on metabolic adaptation processes in *P. aeruginosa*, diverse growth media were selected to simulate distinct lifestyles and to provoke induction of dissimilar metabolic pathways.

Environmental conditions with minimal nutrient supply were imitated by media containing succinate, citrate, glucose or cadaverine as the single carbon source. Out of these media, succinate and citrate are well-established carbon sources for bacteria in *in vitro* cultures (Miller and Ku, 1978; Kirner *et al*., 1996) and known to be preferentially metabolized by *P. aeruginosa* (Ng and Dawes, 1973). Glucose is also widely used as a growth substrate under laboratory conditions, and sugar derivatives are common in the environment; however, glucose represents a less preferred carbon source for *P. aeruginosa*. The catabolism via the Entner-Doudoroff pathway (Entner and Doudoroff, 1952; Goldbourt *et al*., 2007) is less efficient than the glycolysis and is under control of catabolite repression, a global regulatory mechanism allowing hierarchical utilization of carbon sources (Wolff *et al*., 1991; Nishijyo *et al*., 2001; Silo-Suh *et al*., 2005). To mimic bacterial lifestyle under nutrient-poor conditions, the primary amine cadaverine was offered as substrate. As the decarboxylated degradation product of lysine, cadaverine commonly occurs in the environment but allows for only slow and poor growth.

In contrast to single carbon source media, full media mimicked conditions where *P. aeruginosa* inhabits nutrient-rich niches, such as animate hosts or sewage (Mena and Gerba, 2009). In order to analyse adaptation processes to nutrient-rich habitats, which support rapid bacterial growth, these environments were imitated by tryptone and casamino acids media. Both tryptone and casamino acids are derived from casein and have similar amino acid compositions but different complexities. Tryptone is composed of small oligopeptides and requires further hydrolytic degradation prior to metabolization, whereas casamino acids consist of single amino acids.

Specific growth rates of P. aeruginosa

In Fig. 1 the growth curves of three of the six different cultivation conditions are shown. The specific growth rates μ of all conditions were calculated from the exponential growth phase. Specific growth rates in tryptone media were significantly higher [$\mu = 0.85$ (PAO1), $\mu = 0.98$ (TBCF10839)] than in other analysed media. Specific growth rates are comparable in the minimal media succinate, glucose and citrate, whereas in minimal medium with cadaverine specific growth rates for both strains decrease to only 0.17 for PAO1 and 0.15 for TBCF10839. Metabolome analysis was performed during mid-exponential growth and in the stationary growth phase in batch cultures. Samples from mid-exponential growth were taken at $OD_{600} = 1$ (exception: cadaverine $OD_{600} = 0.3$). The second set of samples was taken 2 h after bacterial cultures had entered stationary growth phase, determined by optical density measurement (Fig. 1).

Metabolite analysis of P. aeruginosa

Following GC-MS-based analysis of the *P. aeruginosa* metabolome, 243 compounds were found according to

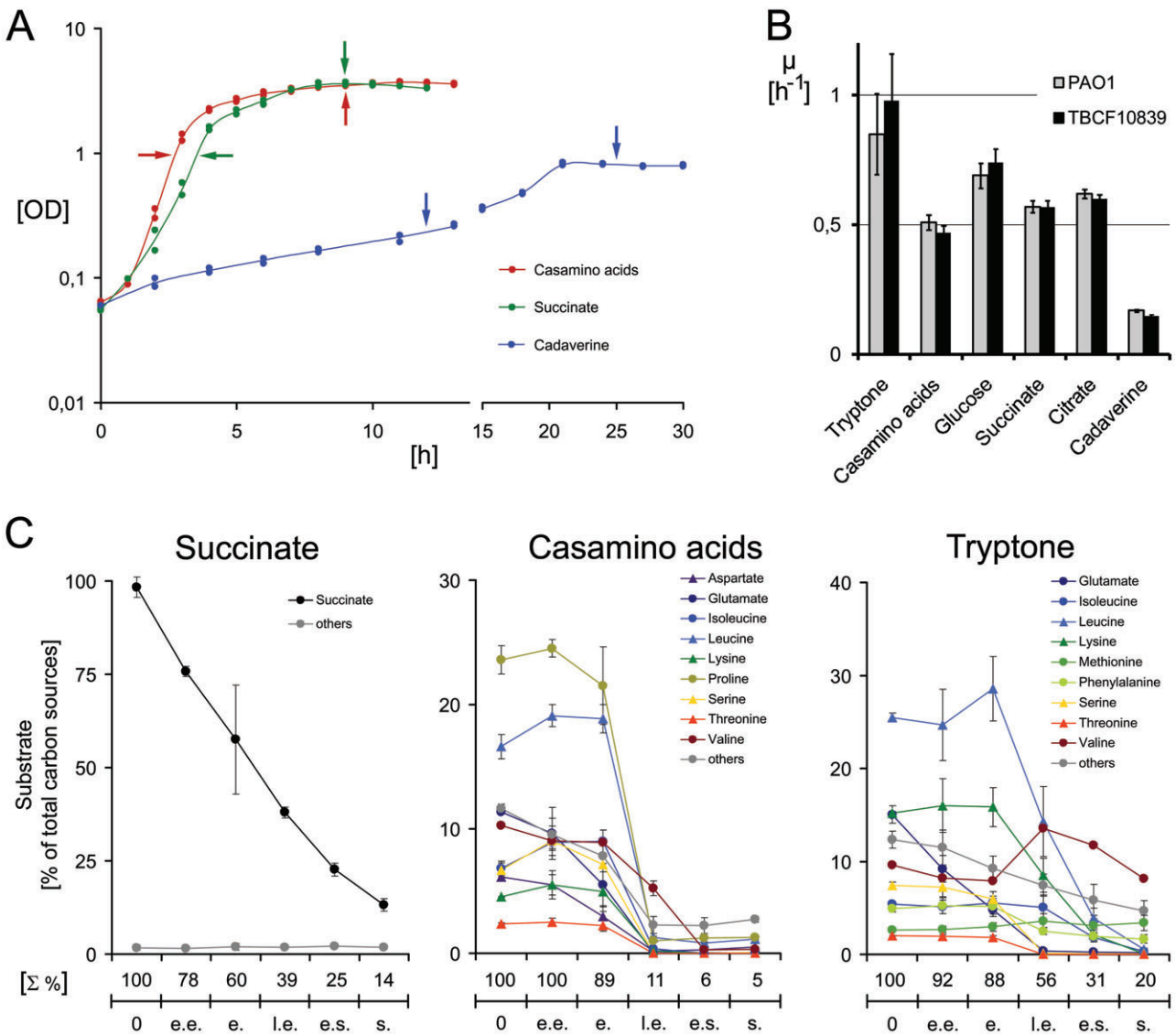

Fig. 1. Growth of *P. aeruginosa* and metabolization of the growth media.
A. Growth curves of *P. aeruginosa* PAO1 on succinate, casamino acids and cadaverine. Growth curves on citrate, tryptone and glucose (data not shown) were comparable to the succinate growth curve. The growth curves of strain TBCF10839 (data not shown) were comparable to the growth curve of PAO1 in the respective medium. In all media, except for cadaverine, both *P. aeruginosa* strains grew exponentially to optical densities > 2. Sampling points for metabolome analysis are indicated by arrows.
B. Growth rates of *P. aeruginosa* strains PAO1 and TBCF10839. Both strains exhibited similar growth rates during exponential growth in the same medium. In cadaverine-containing medium, the growth rate was significantly lower ($P < 0.001$) than in all other analysed media.
C. Metabolization of the growth medium. Supernatant compositions of three different media (succinate, casamino acids and tryptone) incubated with *P. aeruginosa* PAO1 were analysed as representatives, at six time points [start [0], early exponential phase (0.3 OD [e.e.]), exponential phase (1 OD [e.]), late exponential phase (2.0 OD [l.e.]), early stationary phase (3.5 OD [e.s.]), stationary phase (2 h later [s])] to monitor substrate consumption in different growth phases. Carbon compounds that represented less than 2% of the initially nutrients available were grouped as 'others'. In complex growth media, *P. aeruginosa* metabolized nutrients in a specific order. In stationary phase, the succinate- and casamino acid-containing media were depleted of carbon sources, whereas tryptone still contained initial substrates.

their retention times and mass spectra. Out of those, 144 could be matched to known compounds by comparison with our in-house metabolite libraries. Sixty metabolites were found in all analysed conditions, and 64 metabolites were present in most metabolomes, whereas 46 metabolites were only present in a few growth states and media. Nineteen metabolites were exclusively found in single growth conditions, mostly in both *P. aeruginosa* strains.

The majority of identified substances (more than 50%) were represented by metabolites from amino acid and sugar metabolism (Table S1). The number of major metabolites was found to depend on the media composi-

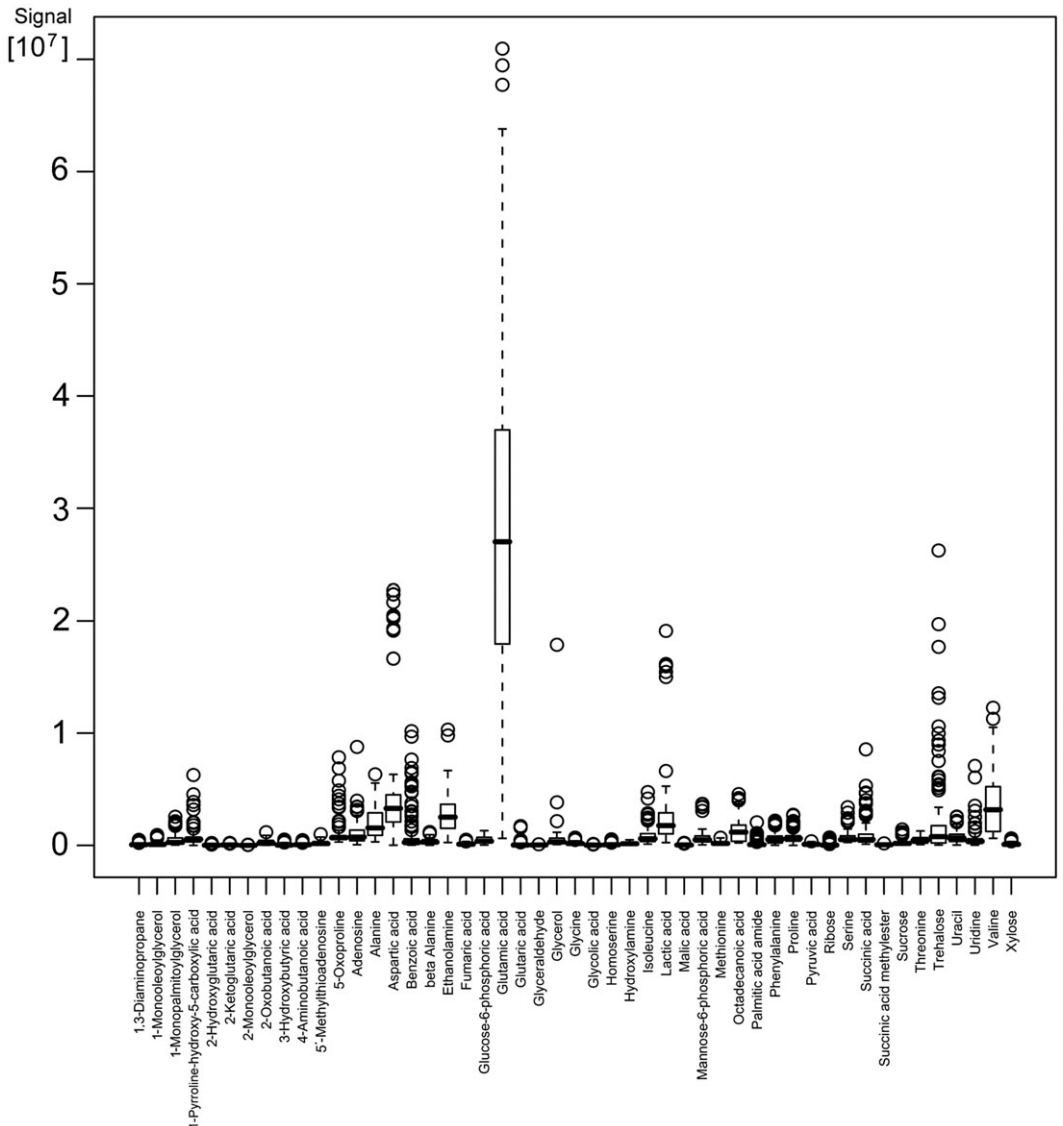

Fig. 2. Box-plot of the concentrations of 49 identified metabolites that were found in all analysed conditions. Glutamate was identified as the compound with the highest mean concentration and variance.

tion, irrespective of growth state. In cadaverine-grown cells, 90% of the total signal intensity of GC analyses was generated by only 22 metabolites with high peak areas (It has to be mentioned here that the relationship between metabolite concentrations and peak areas is compound-specific, i.e. a compound A with a peak area twice the area of compound B is not necessarily present in a higher concentration. On the other hand, a specific metabolite showing a larger peak area in growth condition B compared with A is present in a higher concentration. During the discussion sometimes concentration instead of peak area is used for easier readability). In contrast, in succinate or tryptone media more than 40 metabolites accounted for 90% of the overall signal, indicating a greater diversity of metabolic compounds. In all analysed conditions, a few metabolites prevailed over the overall metabolite spectrum, with glutamate as the most dominant compound (Fig. 2).

According to the Kruskal–Wallis test (analysing significance and reproducibility) for each of the 60 constitutive metabolites at least one or more significant differences between the different media was found (median Chi-square: 105.7, sigma = 9.9; confidence level 0.001: $\pm$ 4.8; median *P*-value: $P = 5 \times 10^{-13}$; Fig. 3, isoleucine as example). Additionally, for each metabolite, concentration alterations between all analysed conditions were tested pairwise in Mann–Whitney *U*-tests. Due to the high technical reproducibility of data and the low biological variance, a large number of significant differences were observed (median 64%, $P < 0.001$ and $P < 0.02$ after cor-

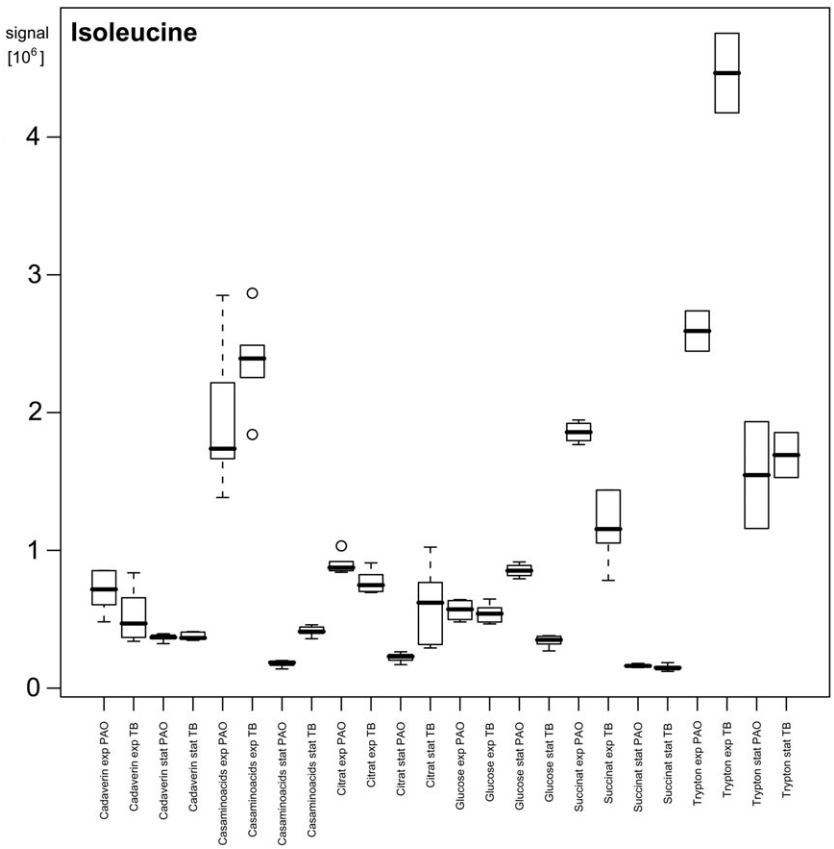

Fig. 3. Box-plot of measured metabolite concentrations for isoleucine (example). The concentration differences between most conditions were significant ($P < 0.001$; $P < 0.02$ after correction for multiple testing).

rection for multiple testing). In other words, the variation of measured data points for each metabolite within one experimental condition were significantly lower compared with results of other conditions.

For a detailed comparison of metabolic states, differences in a metabolite concentration between two conditions were included in the analysis, if the change was statistically significant ($P < 0.02$, corrected Mann–Whitney *U*-test) and at least fourfold up or down. A table with fold-changes of all identified metabolites (normalized to the median signal intensity) was deposited as Table S1.

The fold-changes of metabolite concentrations in different media and growth phases within the same *P. aeruginosa* strain were found to be significantly higher than between different strains in the same medium and growth phase ($P = 4.45 \times 10^{-10}$). This shows that the metabolomes were mostly defined by the growth substrate rather than by the strain-specific genetic background (Fig. 4A). Supporting this hypothesis, under all tested conditions no significant differences between the median fold-changes of metabolite concentrations in strain PAO1 versus strain TBCF10839 were observed ($P = 0.30$) (Fig. 4B).

Analysis of the growth media

In addition to comprehensive analyses of intracellular metabolite profiles, the compositions of growth media were analysed at five time points (Fig. 1) during cultivation in two rich media (tryptone and casamino acids) and in succinate as a representative for minimal media conditions.

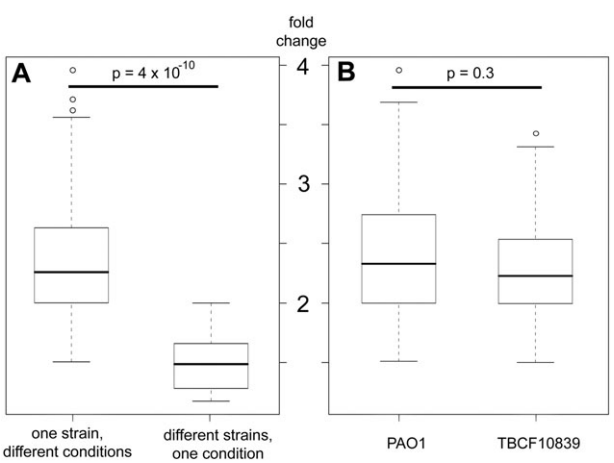

Fig. 4. Comparison of median fold-change of metabolites.
A. Fold-changes of metabolite concentrations between different growth phases within one strain (PAO1 or TBCF10839) were significantly higher ($P = 4.5 \times 10^{-10}$) than the differences between PAO1 and TBCF10839 in the same condition.
B. The median fold-changes of metabolite concentrations were not significantly different ($P = 0.3$) for strain PAO1 and TBCF10839 when different growth conditions were compared for the same strain.

In succinate-containing minimal medium during early exponential growth, *P. aeruginosa* had only the initial carbon source available. In contrast, at later stages of cultivation, virtually all succinate has been metabolized to cytosolic compounds or complex polymers (peptides, polysugars) that were not accessible for GC-MS analysis.

Casamino acids are a mixture of amino acids derived from fully hydrolysed casein. Growing in this medium, *P. aeruginosa* preferentially metabolized compounds that can be easily integrated in central metabolic pathways (Ala, Asp, Glu, Gly, Leu, Pro, Ser, Thr). While most of these compounds were completely digested until mid-exponential growth, other amino acids, which require a more complex catabolism, were metabolized at a later growth state (Ile, Leu, Met, Phe, Tyr, Val). Supernatants from the stationary phase were mostly deprived of the initial carbon source components.

Tryptone is a pancreatic digest of casein/milk powder. It consists mostly of amino acids and oligopeptides, but also contains sugars and lipids. In this complex medium *P. aeruginosa* metabolizes amino acids in the same sequential order as observed in pure casamino acids. Additionally, central carbohydrates (glucose, fructose, glycerol) were also metabolized during the early growth phases, whereas the concentration of other sugars (erythritol, inositol, maltose, mannitol, mannose, ribose, sucrose, trehalose) and fatty acids (dodecanoic acid, hexadecanoic acid, octadecanoic acid) remained nearly unchanged during the whole incubation period. In contrast to other analysed media, tryptone was not completely digested, when *P. aeruginosa* entered the stationary phase.

Principal component analysis

Principal component analysis (PCA) is an orthogonal linear transformation that transforms the data to a new coordinate system such that the greatest variance by any projection of the data comes to lie on the first coordinate, the second greatest variance on the second coordinate, etc. If the first two coordinates represent a large percentage of the whole data variation it allows a visual representation of clustering states.

When a PCA was performed with all identified metabolites and standard parameters, nearly 60% of the total variance was attributed to the first two principal components (data not shown). This high correlation was based on high concentrations of only a few components that dominate the overall variance of the metabolome (e.g. glutamate as the most dominant metabolite caused more than 80% of the total variance in the first two principal components).

In order to overcome the bias caused by the dominance of high-concentration compounds, logarithmically scaled metabolite concentrations were used for the PCA (Fig. 5). The contribution of several dozen metabolites to the first two components explained only 40% of the total variation. However, the examined growth conditions were clearly grouped by nutrient and growth phase, with both of the *P. aeruginosa* strains analysed plotted as nearest neighbours.

Fifty per cent of the first and second principal components were defined by 18% and 23% of the identified metabolites respectively. These two sets of compounds are virtually non-overlapping.

The Eigenvalues of the first principal component (*x*-axis) were mainly determined by metabolites of the gluconeogenesis and the central sugar interconversion. In the second principal component (*y*-axis), metabolites related to growth (aminosugar, nucleotide and lipid metabolism) and degradation of complex amino acids (lysine, aromatic and branched-chain amino acids) were merged (Table 1). A plot of these two principal components represented the overall metabolic state for *P. aeruginosa* in different media: metabolomes reflecting optimal growth with high replication rates and a high sugar metabolism, as observed in tryptone, were located in the upper left corner. Cadaverine, as non-preferred carbon source offered in low concentration, was associated with a massive decrease of many metabolite concentrations, and led to an extreme location in one corner of the PCA plot. The other analysed growth conditions represented three one-carbon source minimal media, as well as CAA medium, which are all rich in substrate concentrations. The corresponding metabolomes from these experiments were located at comparable positions in relation to the *y*-axis; however, variations of their positions on the *x*-axis are indicative of the degree of sugar metabolism in the respective medium.

Hierarchical clustering analysis

In order to illustrate the basic principles of how *P. aeruginosa* metabolically adapts to a specific carbon source or growth phase, logarithmized mean values of metabolite concentrations were analysed in an unsupervized hierarchical cluster analysis (HCA) using Pearson correlation (as current metrics) as similarity measure (Fig. 6).

Two major groups of concentration patterns for the detected metabolites were identified. The first group comprised metabolites that were found in almost all analysed conditions. The concentrations of each of these metabolites were only slightly adapted to varying substrates and growth phases. This finding indicated that *P. aeruginosa* has a stable, nearly invariant core metabolism that is independent of carbon source and growth state. The second group represented metabolites that were found in only a few conditions, for example during exponential and stationary phase of cultures grown on the same carbon

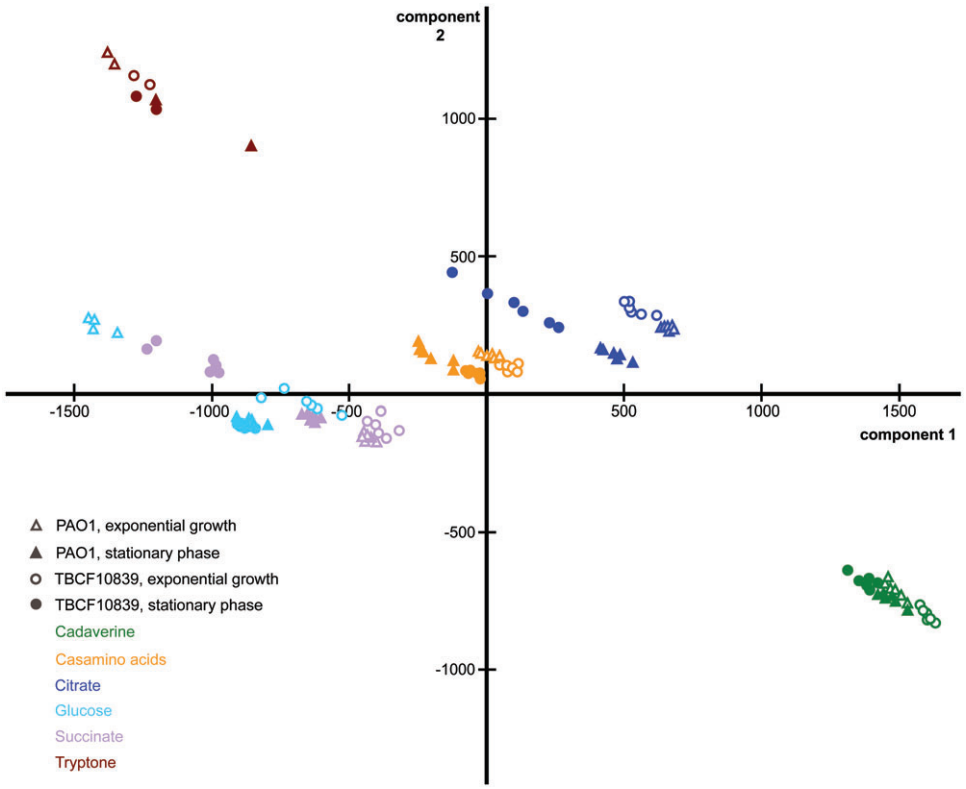

Fig. 5. PCA plot (principal component 1 versus principal component 2) of logarithmically transformed metabolite concentrations from *P. aeruginosa* strains PAO1 and TBCF10839 during exponential growth and in stationary phase growing on various carbon sources. The first two principal components account together for 40% of the variance. The variations of a few highly concentrated metabolites cause more than 80% of the observed effect. The first principal component mainly reflected differences in sugar metabolism, whereas the second represented the overall growth. The metabolomes of strains PAO1 and TBCF10839 from corresponding condition were always closely related.

source. These metabolite spectra were comparable for both strains, which again indicated that variations in the metabolite profile are strongly defined by the environment rather than by the genetic repertoire of different *P. aeruginosa* strains.

Groups of concordantly high concentration metabolites within a given condition revealed metabolic pathways that are used for adaptation to a specific carbon source or growth phase. Enrichment of these metabolites occurred during metabolism and integration of the carbon source into the core metabolism, which leads to the hypothesis that, despite a diverse supply of nutrients, the core metabolism is kept in a stationary state. However, in cadaverine more than 30% of the metabolites found in other analysed conditions were below the detection limit and metabolite concentrations were in general strongly decreased. This finding indicated a strong downregulation of the overall core metabolism in agreement with the decreased growth rate. To enable *P. aeruginosa* for at least very low growth rates on this carbon source (Fig. 1), switching off dispensable pathways and restriction on pivotal metabolic processes might be required.

Altogether, the cluster analysis showed that the observed metabolite spectra were mainly defined by the growth medium. The influence of the growth phase seemed to be less important as in all cases the metabolite spectra of exponential growth and stationary phase were nearest neighbours in the HCA. Clonal differences had the least impact on metabolite patterns as under corresponding growth conditions the strains PAO1 and TBCF10838 always displayed the highest degree of similarity. Our results showed that both strains, regardless of their differences in origin and occupied habitats, share a common, *P. aeruginosa*-specific, carbon source and growth phase-dependent metabolism that is independent of the clonal lineage.

P. aeruginosa *core metabolism*

To define the *P. aeruginosa* core metabolism, all 145 identified metabolites were grouped in metabolic pathways (KEGG database; http://www.genome.jp/kegg/kegg2.html). The subgroup of 60 metabolites found in all analysed conditions was considered as representatives

Table 1. Metabolites with the highest Eigenvalues (determining > 50% of total variance of the first two principal components), grouped in metabolic pathways.

Principal component 1	Principal component 2
Amino acid metabolism	*Amino acid metabolism*
5-Aminopentanoic acid	4-Aminobenzoate
Asparagine	Cadaverine
Citrulline	Cysteine
Homocysteine	Glutamine
	Homocysteine
Lipid metabolism	Leucine
1-Monostearoylglycerol	Lysine
Oleic acid amide	O-Phosphoserine
	Ornithine
Nucleotide metabolism	Phosphoethanolamine
Xanthine	Pipecolinate
	Putrescine
Sugar metabolism	Pyrophosphate
2′-Deoxyguanosine 5′-phosphate	Pyrrole-2-carboxylate
2-Phosphoglycerate	Spermidine
Arabinose	Tyrosine
Erythritol	
Glucose-1-phosphate	*Lipid metabolism*
Glycerone phosphate	Glycerol-3-phosphate
Glyoxylic acid	3-Phosphoglycerate
Isomaltose	Tetradecanol
Phosphoenolpyruvate	Hexadecanol
Pyrophosphate	Hexadecanoate
Ribulose-5-phosphate	Dodecanoate
Uridine-5′-monophosphate	
Xylulose	*Nucleotide metabolism*
	Adenine
	Adenosine-5′-monophosphate
	Hypoxanthine
	(Amino-) Sugar- and Nucleoside metabolism
	1,6-Anhydro-beta-D-glucose
	Glucono lactone
	Glucosamine
	Glucose
	Mannitol
	Mannose
	N-Acetyl-glutamic acid
	Ribose-5-phosphoric acid
	Xylitol
	Xylulose-5-phosphoric acid
	Central metabolism
	Citric acid
	Diethylene glycol
	Nicotinic acid

for a stably utilized core metabolism. Pathways containing metabolites of this group (significantly above average) were assigned to the core metabolism (Table 2, *P*-values were calculated by Monte Carlo simulation). As expected, the identified metabolic pathways belonged to the central amino acid and energy metabolism.

In the metabolite analysis, glutamate was identified as the compound with the highest concentration and variance in *P. aeruginosa*, dominating the metabolite spectrum (Fig. 2). This metabolite is part of or closely related to those pathways that were assigned to the core metabolism with high significance. Together with the observation that – independent of the growth condition – the concentrations of most metabolites were kept at nearly constant levels (Fig. 6), these findings suggested that glutamate and the related pathways may play a crucial role for the *P. aeruginosa* metabolism. The high concentration of glutamate allows *P. aeruginosa* to interconnect diverse pathways and to use this central metabolite as a universal substrate for various anabolic and catabolic processes.

Adaptation of P. aeruginosa *to diverse carbon sources*

Metabolic adaptation of *P. aeruginosa* was analysed by separate normalization and subsequent cluster analysis (Fig. 7). According to the previous HCA result, the metabolite patterns of strains PAO1 and TBCF10839 were defined by the growth condition. The most striking observation was the increase of distinct subsets of metabolites in a growth condition-characteristic manner. These sets of metabolites with high abundance reflected metabolic pathways that were specifically utilized by *P. aeruginosa* during metabolic adaptation to the respective medium and/or growth phase serving to integrate the available carbon source in a mainly unaltered background metabolism.

As expected, metabolites that were directly available as carbon sources and those belonging to the central catabolic pathways of the growth substrate were found in higher concentrations during exponential growth. In the stationary phase, with most growth media depleted from initial carbon sources, the metabolite pattern were more complex than during exponential growth. Stationary phase metabolomes were enriched with metabolites associated with sugar metabolism suggesting induced adaptation to stationary growth with, e.g. enhanced production of exopolysaccharides, development of biofilms, and production of rhamnolipids. Additionally, at high cell densities the nutrient-poor conditions led to degradation

Table 2. Metabolic pathways in the invariant core metabolism.

Overrepresented (in constitutive detected metabolites)	
Pathway	*P*-value
Butanoate Metabolism	0.00001
Alanine, Aspartate and Glutamate Metabolism	0.00098
Cysteine and Methionine Metabolism	0.00683
Phenylalanine Metabolism	0.00871
Valine, Leucine and Isoleucine Biosynthesis	0.00907
Citrate Cycle	0.02059
Cyanamino Acid Metabolism	0.02466

Identified metabolites were grouped to metabolic pathways (according to KEGG database, http://www.genome.jp/kegg/kegg2.html), metabolites that were found in all analysed growth conditions (core metabolites) were significantly overrepresented in a set of central metabolic pathways. No pathways were found with a significant underrepresentation of these core metabolites.

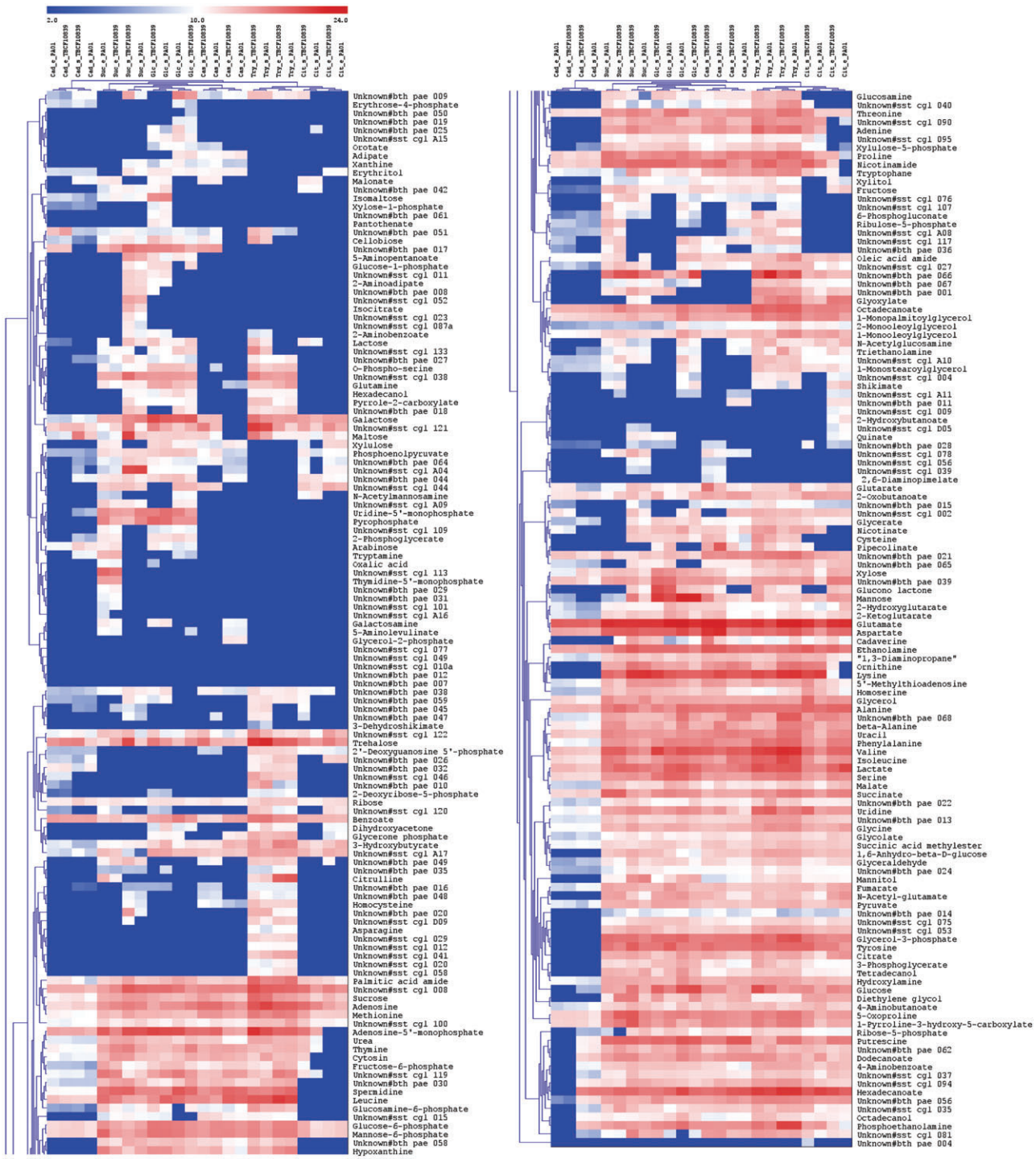

Fig. 6. Unsupervised hierarchical clustering of the logarithmically transformed into (log2) metabolite concentrations of all 243 found metabolites. The metabolites were divided in two groups: (i) metabolites that were constitutively present and (ii) metabolites that appeared in dependence of the growth conditions. Qualitative differences between both analysed *P. aeruginosa* strains were rare [Growth substrates: cadaverine (Cad); casamino acids (Cas); citrate (Cit); glucose (Glc); succinate (Suc); tryptone (Try). Growth phase: (e)xponential and (s)tationary. Strains: PAO1 and TBCF10839].

Fig. 7. Hierarchical clustering of the normalized metabolite concentrations of all 243 found metabolites. To illustrate the relative concentration changes of each metabolite, a heat map was generated based on relative metabolite concentration of a given sample compared with the mean of the concentration values across all samples for the given growth condition. This plot shows that, in a condition specific fashion, sets of metabolites were increased [Growth substrates: cadaverine (Cad); casamino acids (Cas); citrate (Cit); glucose (Glc); succinate (Suc); tryptone (Try). Growth phase: (e)xponential and (s)tationary. Strains: PAO1 and TBCF10839].

of less preferred amino acids (e.g. Lys, Phe, Trp, Tyr), the catabolic intermediates of which were overrepresented in the stationary state metabolomes.

This common metabolic pattern is flanked by two extremes: the growth in tryptone and cadaverine. In tryptone, as the most complex and nutrient-rich medium, the largest group of high concentration metabolites was found. *Pseudomonas aeruginosa* entered the stationary phase prior to metabolizing supplied media components (Fig. 1) and thus still had access to diverse nutrients in late growth phases. Consequently, the bacterial metabolomes of exponential growth and stationary phase were closely related and reflected an adaptation to conditions with a rich and diverse nutrient range. Metabolomes in tryptone were dominated by many highly concentrated metabolites of sugar and amino acid metabolism that superimposed on metabolites of the background metabolism. This effect was not observed in other media and thus resulted in clustering of metabolomes from tryptone-grown cells as outliers in the HCA (Fig. 7).

Cadaverine-grown cells also exhibited closely related metabolomes from exponential growth and stationary phase. However, in this case the insufficient carbon source evoked a fourfold extension of generation time, and these low growth rates were reflected by a metabolome state with the overall lowest metabolite concentrations. The high similarities in the metabolomes of exponential growth and stationary phase were caused by substrate limitations in both growth phases.

Although most analysed media (exception tryptone) reach a similar, nutrient-depleted state in the stationary phase (Fig. 1), the metabolomes of *P. aeruginosa* strains in this late growth phase were still biased by the initial substrate conditions. Maintaining the substrate-characteristic metabolite patterns under nutrient-poor conditions might reflect the corresponding enzymatic repertoire, which has been retained mainly unchanged, too. It is well known that enzymatic adaptation to a carbon source is often induced by the growth substrate itself (Lee *et al*., 2008; Boulette *et al*., 2009). This specified adaptation process appears to be only slowly reversed under food-limiting conditions as indicated by reduced lag phases if inoculates had been grown on the same substrate.

Conclusion

The analysis of the *P. aeruginosa* metabolome revealed specified metabolic responses that arise in a nutrition-dependent manner. As previously reported for *Pseudomonas putida* (van der Werf *et al*., 2008) induction of substrate-specific metabolic pathways (represented by distinct sets of metabolites) indicates the precise regulation of adaptation processes. Beside this adaptive response, a basic core metabolism shapes the *P. aeruginosa* metabolome independent of growth phase, carbon source or clonal variations.

Experimental procedures

Pseudomonas aeruginosa *strains*

All experiments were performed with two distantly related, genetically and phenotypically well-characterized *P. aeruginosa* isolates. Strain PAO1 (genotype 0002) was isolated in 1955 in Melbourne, Australia, from an infected wound (Holloway, 1955) and is the sequenced major reference strain widely used in *P. aeruginosa* research (Stover *et al*., 2000). Strain TBCF10839 (genotype 3C52) (Wiehlmann *et al*., 2007a) was isolated in the early eighties in Hannover from a chronically colonized cystic fibrosis patient (Wiehlmann *et al*., 2007b). It is a mucoid strain, harbouring a *mucA* nucleotide substitution [A342G, compared with strain PAO1 sequence (http://www.pseudomonas.com), which, however, does not lead to loss of function (J. Klockgether, pers. comm.).

Media and cultivation

For metabolome analysis precultures and main cultures of *P. aeruginosa* strains PAO1 and TBCF10839 were grown in either minimal medium [2 g l^{-1} $(NH_4)_2SO_4$, 4 g l^{-1} Na_2HPO_4, 3 g l^{-1} KH_2PO_4, 3 g l^{-1} NaCl] with trace metals (0.49 g l^{-1} $MgSO_4 \times 7H_2O$, 0.04 g l^{-1} $CaCl_2 \times 6H_2O$, 20 μg l^{-1} $MnCl_2 \times 4H_2O$, 20 μg l^{-1} $CuSO_4$, 20 μg l^{-1} $ZnSO_4 \times 7H_2O$, 10 μg l^{-1} $Na_2MoO_4 \times 2H_2O$, 2.8 μg l^{-1} $FeSO_4 \times 7H_2O$) containing a sole carbon source [40 mM succinate (Roth), 40 mM citrate (Sigma), 40 mM glucose (Roth), 5 mM cadaverine (Sigma) or 1% casamino acids (Roth)] or in complex media containing tryptone (AppliChem) (20 g l^{-1})/NaCl (10 g l^{-1}).

All cultivations were carried out at 37°C and 250 r.p.m. on a rotary shaker in triplicate.

For adequate aeration baffled shake flasks (500 ml) were used with 150 ml of culture medium.

The specific growth rates μ were calculated according to Berney and colleagues (2006) ($\mu = \Delta \ln OD/\Delta t$).

Metabolome analysis

Intracellular metabolites. For sampling of intracellular metabolites 150 mg of cells (wet weight) was harvested by centrifugation (5000 *g*, 4°C, 5 min) and the media supernatant was removed.

Extraction of intracellular metabolites was performed as described by Haddad and colleagues (2009). Briefly, the following steps were carried out at 4°C. Obtained cell pellets were washed twice with 20 ml of 0.9% NaCl solution and finally resuspended in 1.5 ml methanol containing 40 μl ribitol (0.2 g l^{-1}) per ml methanol as internal standard. The cells were disrupted by ultrasonification (15 min, 70°C). 1.5 ml H_2O was added and samples were thoroughly mixed for 30 s. The addition of 1 ml chloroform was followed by mixing and subsequent centrifugation (4000 *g*, 4°C, 10 min) for separation of hydrophilic and hydrophobic phases. One millilitre of the polar phase was transferred to a new reaction tube and dried.

For derivatization dried samples were dissolved in 50 μl pyridine containing methoxyamine hydrochloride (20 mg ml^{-1}) and incubated at 600 r.p.m. and 30°C for 90 min. After adding 80 μl N-methyl-N-trimethylsilyltrifluoracetamide (Chromatographie Service, Langerwehe, Germany) samples were incubated again (600 r.p.m., 37°C, 30 min) followed by another 120 min incubation at 20°C.

Finally, 6 μl of an alkane mix containing decane, dodecane, pentadecane, nonadecane, docosane, octacosane, dotriacontane and hexatriacontane (20 mg ml^{-1} in cyclohexane each) was added in order to allow retention indices calculations (Vandendool and Kratz, 1963; Strelkov *et al*., 2004).

A sample aliquot of 2 μl was injected in a Finnigan Trace gas chromatograph (ThermoFinnigan, San Jose, USA) equipped with a DB-5MS column (J&W Scientific, Folsom, USA). Eluted compounds were analysed with a Trace mass spectrometer (ThermoFinnigan, San Jose, USA) after electron impact ionization. Applied parameters for sample injection, gas chromatography and mass spectrometry were described before (Strelkov *et al*., 2004). The metabolite identification and quantification were previously described (Strelkov *et al*., 2004; Spura *et al*., 2009).

Extracellular metabolites. For studying the extracellular metabolites, 10 ml of supernatants was taken at the particular time points. The metabolites were extracted at 4°C. The bacterial cells were removed by centrifugation (2× 6000 *g*, 5 min, 4°C) and an aliquot of the upper part of the centrifuged supernatant was used for metabolome analysis.

The supernatant was diluted 20-fold with water. An aliqout of 1 ml was mixed with 1.5 ml of methanol, containing 12 μg of ribitol as internal standard. The samples were mixed for 60 s. 1 ml chloroform was added and hydrophilic and hydrophobic phases were separated by centrifugation (4000 *g*, 4°C, 5 min); 1 ml of the polar phase was transferred to a new tube and dried.

For derivatization, dried samples were solved in 40 μl pyridine, containing methoxyamine hydrochloride (20 mg ml^{-1}) and incubated at 600 r.p.m. and 30°C for 90 min. After adding 70 μl of N-methyl-N-trimethylsilytrifluoroacetamide samples were incubated again (600 r.p.m., 37°C, 30 min) followed by another incubation (600 r.p.m., 25°C, 120 min) and centrifugation (18 000 *g*, 20°C, 5 min). The GC-MS analysis was performed with the supernatant (after addition of the abovementioned alkane standard).

Statistical analysis

Generally, all metabolome analysis experiments were performed with six replicates (tryptone samples were analysed in duplicates as the macromolecular components of this medium may cause damages of the GC column). Metabolite concentrations were scaled to the internal standard ribitol and to the optical density of cell culture and then calibrated to total signal intensity of the GC spectra. Metabolite concentrations below the detection limit were set to the lowest measured signal. Median intensity values of the six replicates were applied to statistical analysis. Statistical tests for significance (Kruskal–Wallis and Wilcoxon–Mann–Whitney tests) were performed with the R package (http://www.r-project.org/; Gentleman *et al*., 2005; R Development Core Team, 2008). Non-random pathway-metabolite association was tested by Monte Carlo simulations (Sham and Curtis, 1995).

Principal component analysis

Principal component analysis is a non-parametric method used for pattern recognition requiring no *a priori* knowledge of data structure. This technique is designed to simplify data sets by reducing the dimensionality of the multivariate data. The resulting compressed data preserve the relevant features of the original data set, which are represented by a set of new variables, termed principal components. Briefly, PCA classifies data sets of unknown structure into meaningful groups. In this analysis standard parameters implemented in the TIGR Mev software (http://www.tm4.org/mev, Eisen *et al*., 1998) were used. The PCA based on logarithmic calculus was performed simultaneously for all data sets. The principle component calculations were performed with a Centering Mode based on mean.

Unsupervised hierarchical clustering (HCA)

This method provides organization of primary data sets without predefined classification. Based on similarity, clustering of samples as well as associated signature features of sample are visualized by dendrograms. Analysis was performed simultaneously for all data sets. The HCA was based upon logarithmic calculus implemented in the TIGR Mev software. Mean centred values were normalized for metabolite/row, and where required for condition/column. Pearson correlation was used as similarity metric for the HCA.

Acknowledgements

We would like to thank Colin Davenport for assistance with statistical analyses; and Burkhard Tuemmler for stimulating discussions during the preparation of this manuscript. S.H. receives a predoctoral Lichtenberg stipend by the Niedersächsisches Ministerium für Wissenschaft und Kultur and financial support by the DFG-funded Hannover Biomedical Research School. L.W. is supported by a competitive research grant provided by Hannover Medical School (HLF04/08).

References

Anba, J., Bidaud, M., Vasil, M.L., and Lazdunski, A. (1990) Nucleotide sequence of the *Pseudomonas aeruginosa* phoB gene, the regulatory gene for the phosphate regulon. *J Bacteriol* **172:** 4685–4689.

Berney, M., Weilenmann, H.U., Ihssen, J., Bassin, C., and Egli, T. (2006) Specific growth rate determines the sensitivity of *Escherichia coli* to thermal, UVA, and solar disinfection. *Appl Environ Microbiol* **72:** 2586–2593.

Boulette, M.L., Baynham, P.J., Jorth, P.A., Kukavica-Ibrulj, I., Longoria, A., Barrera, K., *et al*. (2009) Characterization of alanine catabolism in *Pseudomonas aeruginosa* and its importance for proliferation *in vivo*. *J Bacteriol* **191:** 6329–6334.

Campa, M., Bendinelli, M., and Friedman, H. (eds) (1993) *Pseudomonas Aeruginosa as an Opportunistic Pathogen*. New York, NY, USA: Plenum Press.

Davies, D.G., Chakrabarty, A.M., and Geesey, G.G. (1993) Exopolysaccharide production in biofilms: substratum activation of alginate gene expression by *Pseudomonas aeruginosa*. *Appl Environ Microbiol* **59:** 1181–1186.

Davies, K.J., Lloyd, D., and Boddy, L. (1989) The effect of oxygen on denitrification in Paracoccus denitrificans and *Pseudomonas aeruginosa*. *J Gen Microbiol* **135:** 2445–2451.

Eisen, M.B., Spellman, P.T., Brown, P.O., and Botstein, D. (1998) Cluster analysis and display of genome-wide expression patterns. *Proc Natl Acad Sci USA* **95:** 14863–14868.

Entner, N., and Doudoroff, M. (1952) Glucose and gluconic acid oxidation of *Pseudomonas saccharophila*. *J Biol Chem* **196:** 853–862.

Eschbach, M., Schreiber, K., Trunk, K., Buer, J., Jahn, D., and Schobert, M. (2004) Long-term anaerobic survival of the opportunistic pathogen *Pseudomonas aeruginosa* via pyruvate fermentation. *J Bacteriol* **186:** 4596–4604.

Filiatrault, M.J., Picardo, K.F., Ngai, H., Passador, L., and Iglewski, B.H. (2006) Identification of *Pseudomonas aeruginosa* genes involved in virulence and anaerobic growth. *Infect Immun* **74:** 4237–4245.

Gallagher, L.A., and Manoil, C. (2001) *Pseudomonas aeruginosa* PAO1 kills Caenorhabditis elegans by cyanide poisoning. *J Bacteriol* **183:** 6207–6214.

Gentleman, R., Carey, V., Huber, W., Irizarry, R., and Dudoit, S. (eds) (2005) *Bioinformatics and Computational Biology Solutions Using R and Bioconductor. Statistics for Biology and Health.* New York, NY, USA: Springer.

Gjersing, E.L., Herberg, J.L., Horn, J., Schaldach, C.M., and Maxwell, R.S. (2007) NMR metabolomics of planktonic and biofilm modes of growth in *Pseudomonas aeruginosa*. *Anal Chem* **79:** 8037–8045.

Goldbourt, A., Day, L.A., and McDermott, A.E. (2007) Assignment of congested NMR spectra: carbonyl backbone enrichment via the Entner-Doudoroff pathway. *J Magn Reson* **189:** 157–165.

Haddad, I., Hiller, K., Frimmersdorf, E., Benkert, B., Schomburg, D., and Jahn, D. (2009) An emergent self-organizing map based analysis pipeline for comparative metabolome studies. *In Silico Biol* **9:** 16.

Hickey, W.J., and Focht, D.D. (1990) Degradation of mono-, di-, and trihalogenated benzoic acids by *Pseudomonas aeruginosa* JB2. *Appl Environ Microbiol* **56:** 3842–3850.

Holloway, B.W. (1955) Genetic recombination in *Pseudomonas aeruginosa*. *J Gen Microbiol* **13:** 572–581.

Kiewitz, C., and Tümmler, B. (2000) Sequence diversity of *Pseudomonas aeruginosa*: impact on population structure and genome evolution. *J Bacteriol* **182:** 3125–3135.

Kirner, S., Krauss, S., Sury, G., Lam, S.T., Ligon, J.M., and van Pée, K.H. (1996) The non-haem chloroperoxidase from *Pseudomonas fluorescens* and its relationship to pyrrolnitrin biosynthesis. *Microbiology* **142:** 2129–2135.

Krieger, R., Rompf, A., Schobert, M., and Jahn, D. (2002) The *pseudomonas aeruginosa* hemA promoter is regulated by Anr, Dnr, NarL and integration host factor. *Mol Genet Genomics* **267:** 409–417.

Lee, S.J., Lewis, D.E.A., and Adhya, S. (2008) Induction of the galactose enzymes in *Escherichia coli* is independent of the C-1-hydroxyl optical configuration of the inducer d-galactose. *J Bacteriol* **190:** 7932–7938.

Leisinger, T., and Margraff, R. (1979) Secondary metabolites of the fluorescent pseudomonads. *Microbiol Rev* **43:** 422–442.

Lessie, T.G., and Neidhardt, F.C. (1967) Formation and operation of the histidine-degrading pathway in *Pseudomonas aeruginosa*. *J Bacteriol* **93:** 1800–1810.

Marín, M.M., Yuste, L., and Rojo, F. (2003) Differential expression of the components of the two alkane hydroxylases from *Pseudomonas aeruginosa*. *J Bacteriol* **185:** 3232–3237.

Meile, L., Soldati, L., and Leisinger, T. (1982) Regulation of proline catabolism in *Pseudomonas aeruginosa* PAO. *Arch Microbiol* **132:** 189–193.

Mena, K.D., and Gerba, C.P. (2009) Risk assessment of *Pseudomonas aeruginosa* in water. *Rev Environ Contam Toxicol* **201:** 71–115.

Miller, R.V., and Ku, C.M. (1978) Characterization of *Pseudomonas aeruginosa* mutants deficient in the establishment of lysogeny. *J Bacteriol* **134:** 875–883.

Ng, F.M., and Dawes, E.A. (1973) Chemostat studies on the regulation of glucose metabolism in *Pseudomonas aeruginosa* by citrate. *Biochem J* **132:** 129–140.

Nishijyo, T., Haas, D., and Itoh, Y. (2001) The CbrA-CbrB two-component regulatory system controls the utilization of multiple carbon and nitrogen sources in *Pseudomonas aeruginosa*. *Mol Microbiol* **40:** 917–931.

OECD (1997) *Consensus Document on Information Used in the Assessment of Environmental Applications Involving Pseudomonas*. Series on Harmonization of Regulatory Oversight in Biotechnology, No. 6. Paris, France: OECD.

Palleroni, N.J. (1986) Taxonomy of *Pseudomonads*. In *The Bacteria, Volume X; The Biology of Pseudomonas*. Sokatch, J.R. (ed.). London, UK: Academic Press, pp. 3–25.

Palma, M., Worgall, S., and Quadri, L.E.N. (2003) Transcriptome analysis of the *Pseudomonas aeruginosa* response to iron. *Arch Microbiol* **180:** 374–379.

Quinn, J.P. (2003) *Pseudomonas aeruginosa* infections in the intensive care unit. *Semin Respir Crit Care Med* **24:** 61–68.

R Development Core Team (2008) *R: A Language and Environment for Statistical Computing*. Vienna, Austria: R Foundation for Statistical Computing.

Ramos, J.-L. (ed.) (2004) *Volume 1: Genomics, Life Style and Molecular Architecture*. New York, NY, USA: Kluwer Academic/Plenum Publishers, pp. 369–571.

Salunkhe, P., Töpfer, T., Buer, J., and Tümmler, B. (2005) Genome-wide transcriptional profiling of the steady-state response of *Pseudomonas aeruginosa* to hydrogen peroxide. *J Bacteriol* **187:** 2565–2572.

Schmidt, K.D., Tümmler, B., and Römling, U. (1996) Comparative genome mapping of *Pseudomonas aeruginosa* PAO with *P. aeruginosa* C, which belongs to a major clone in cystic fibrosis patients and aquatic habitats. *J Bacteriol* **178:** 85–93.

Sham, P.C., and Curtis, D. (1995) Monte Carlo tests for associations between disease and alleles at highly polymorphic loci. *Ann Hum Genet* **59:** 97–105.

Silo-Suh, L., Suh, S.-J., Phibbs, P.V., and Ohman, D.E. (2005) Adaptations of *Pseudomonas aeruginosa* to the cystic fibrosis lung environment can include deregulation of zwf, encoding glucose-6-phosphate dehydrogenase. *J Bacteriol* **187:** 7561–7568.

Spura, J., Reimer, L.C., Wieloch, P., Schreiber, K., Buchinger, S., and Schomburg, D. (2009) A method for enzyme quenching in microbial metabolome analysis successfully applied to gram-positive and gram-negative bacteria and yeast. *Anal Biochem* **394:** 192–201.

Stanier, R.Y., Palleroni, N.J., and Doudoroff, M. (1966) The aerobic pseudomonads: a taxonomic study. *J Gen Microbiol* **43:** 159–271.

Stover, C.K., Pham, X.Q., Erwin, A.L., Mizoguchi, S.D., Warrener, P., Hickey, M.J., *et al*. (2000) Complete genome sequence of *Pseudomonas aeruginosa* PAO1, an opportunistic pathogen. *Nature* **406:** 959–964.

Strelkov, S., von Elstermann, M., and Schomburg, D. (2004) Comprehensive analysis of metabolites in Corynebacterium glutamicum by gas chromatography/mass spectrometry. *Biol Chem* **385:** 853–861.

Suh, S.-J., Runyen-Janecky, L.J., Maleniak, T.C., Hager, P., MacGregor, C.H., Zielinski-Mozny, N.A., *et al*. (2002) Effect of vfr mutation on global gene expression and catabolite repression control of *Pseudomonas aeruginosa*. *Microbiology* **148:** 1561–1569.

Trautmann, M., Lepper, P.M., and Haller, M. (2005) Ecology of *Pseudomonas aeruginosa* in the intensive care unit and the evolving role of water outlets as a reservoir of the organism. *Am J Infect Control* **33:** S41–S49.

Tricot, C., Wauven, C.V., Wattiez, R., Falmagne, P., and Stalon, V. (1994) Purification and properties of a succinyltransferase from *Pseudomonas aeruginosa* specific for both arginine and ornithine. *Eur J Biochem* **224:** 853–861.

Vandendool, H., and Kratz, P.D. (1963) A generalization of the retention index system including linear temperature programmed gas-liquid partition chromatography. *J Chromatogr* **11:** 463–471.

Wauven, C.V., Piérard, A., Kley-Raymann, M., and Haas, D. (1984) *Pseudomonas aeruginosa* mutants affected in anaerobic growth on arginine: evidence for a four-gene cluster encoding the arginine deiminase pathway. *J Bacteriol* **160:** 928–934.

Weir, T.L., Stull, V.J., Badri, D., Trunck, L.A., Schweizer, H.P., and Vivanco, J. (2008) Global gene expression profiles suggest an important role for nutrient acquisition in early pathogenesis in a plant model of *Pseudomonas aeruginosa* infection. *Appl Environ Microbiol* **74:** 5784–5791.

van der Werf, M.J., Overkamp, K.M., Muilwijk, B., Koek, M.M., van der Werff-van der Vat, B.J.C., Jellema, R.H., *et al*. (2008) Comprehensive analysis of the metabolome of *Pseudomonas putida* S12 grown on different carbon sources. *Mol Biosyst* **4:** 315–327.

Wiehlmann, L., Munder, A., Adams, T., Juhas, M., Kolmar, H., Salunkhe, P., and Tümmler, B. (2007a) Functional genomics of *Pseudomonas aeruginosa* to identify habitat-specific determinants of pathogenicity. *Int J Med Microbiol* **297:** 615–623.

Wiehlmann, L., Wagner, G., Cramer, N., Siebert, B., Gudowius, P., Morales, G., *et al*. (2007b) Population structure of *Pseudomonas aeruginosa*. *Proc Natl Acad Sci USA* **104:** 8101–8106.

Williams, H.D., Zlosnik, J.E.A., and Ryall, B. (2007) Oxygen, cyanide and energy generation in the cystic fibrosis pathogen *Pseudomonas aeruginosa*. *Adv Microb Physiol* **52:** 1–71.

Wolff, J.A., MacGregor, C.H., Eisenberg, R.C., and Phibbs, P.V. (1991) Isolation and characterization of catabolite repression control mutants of *Pseudomonas aeruginosa* PAO. *J Bacteriol* **173:** 4700–4706.

Supporting information

Additional Supporting Information may be found in the online version of this article:

Table S1. Fold-changes of all identified metabolites, normalized to their median signal intensity.

Please note: Wiley-Blackwell are not responsible for the content or functionality of any supporting materials supplied by the authors. Any queries (other than missing material) should be directed to the corresponding author for the article.